

Hit from both sides: tracking industrial and volcanic plumes in Mexico City with surface measurements and OMI SO₂ retrievals during the MILAGRO field campaign

B. de Foy¹, N. A. Krotkov², N. Bei^{3,4}, S. C. Herndon⁵, L. G. Huey⁶, A.-P. Martínez⁷, L. G. Ruiz-Suárez⁸, E. C. Wood⁵, M. Zavala^{3,4}, and L. T. Molina^{3,4}

¹Department of Earth and Atmospheric Sciences, Saint Louis University, St. Louis, MO, USA

²Goddard Earth Sciences and Technology Center, University of Maryland, MD, USA

³Molina Center for Energy and the Environment, La Jolla, CA, USA

⁴Department of Earth, Atmospheric and Planetary Sciences, Massachusetts Institute of Technology, Cambridge, MA, USA

⁵Aerodyne Research Inc., Billerica, MA, USA

⁶Georgia Institute of Technology, Atlanta, GA, USA

⁷General Direction of the National Center for Environmental Research and Training (CENICA), National Institute of Ecology (INE), Mexico

⁸Centro de Ciencias de la Atmósfera, Universidad Nacional Autónoma de México, Mexico

Received: 17 July 2009 – Published in Atmos. Chem. Phys. Discuss.: 6 August 2009

Revised: 3 December 2009 – Accepted: 4 December 2009 – Published: 22 December 2009

Abstract. Large sulfur dioxide plumes were measured in the Mexico City Metropolitan Area (MCMA) during the MILAGRO field campaign. This paper seeks to identify the sources of these plumes and the meteorological processes that affect their dispersion in a complex mountain basin. Surface measurements of SO₂ and winds are analysed in combination with radar wind profiler data to identify transport directions. Satellite retrievals of vertical SO₂ columns from the Ozone Monitoring Instrument (OMI) reveal the dispersion from both the Tula industrial complex and the Popocatepetl volcano. Oversampling the OMI swath data to a fine grid (3 by 3 km) and averaging over the field campaign yielded a high resolution image of the average plume transport. Numerical simulations are used to identify possible transport scenarios. The analysis suggests that both Tula and Popocatepetl contribute to SO₂ levels in the MCMA, sometimes on the same day due to strong vertical wind shear. During the field campaign, model estimates suggest that the volcano accounts for about one tenth of the SO₂ in the MCMA, with a roughly equal split for the rest between urban sources and the Tula industrial complex. The evaluation of simulations with known sources and pollutants suggests that the combination

of observations and meteorological models will be useful in identifying sources and transport processes of other plumes observed during MILAGRO.

1 Introduction

Sulfur dioxide (SO₂) might well be thought to be the least of Mexico City's air quality problems. And yet, two large point sources on either side of the urban area provide a natural experiment in basin dispersion and a valuable tracer for wind transport in the region. Tracking the movement of SO₂ in the basin reveals meteorological features that are difficult to observe directly, and it identifies transport episodes for use in interpreting measurements made during the MILAGRO field campaign.

1.1 SO₂ emissions and detection

The Mexico City Metropolitan Area (MCMA) lies in an elevated basin surrounded by mountains with an opening to the Mexican Plateau to the north, and is home to over 20 million people. The MILAGRO field campaign took place in March 2006 to characterise the atmospheric pollution in the basin and the export and transformation of pollutants to the



Correspondence to: B. de Foy
(bdefoy@slu.edu)

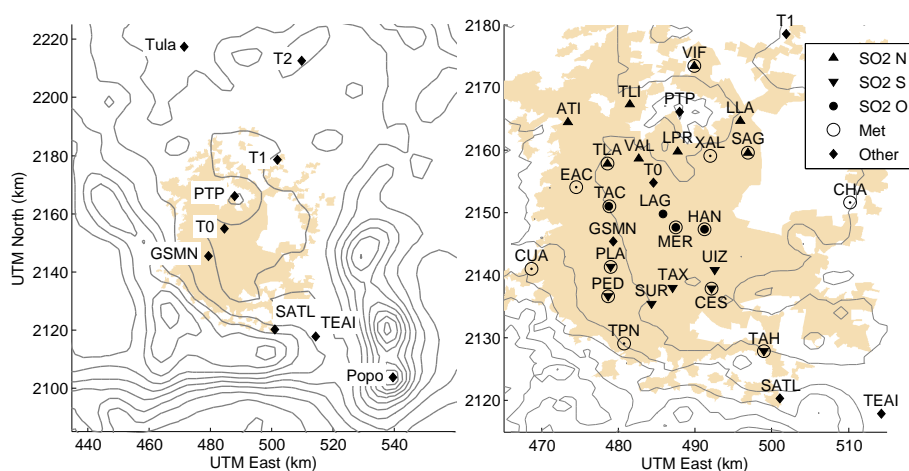


Fig. 1. Map of the basin and the MCMA showing sites used in this study. RAMA SO₂ and meteorology sites shown on the right, classified by groups used for plotting (N=North, S=South, O=Central). Urban area of the MCMA shown in beige, terrain contours every 250 m.

surrounding regions as a way of evaluating possible megacity impacts on the global atmosphere and climate.

The Popocatepetl volcano is a passively degassing eruptive volcano rising to 5426 m m.s.l. which forms part of the southeastern rim of the Mexico City basin and is approximately 70 km southeast of the MCMA centre. It emits SO₂ continuously in the absence of any visible eruptions (Delgado-Granados et al., 2001). During the MILAGRO field campaign, Grutter et al. (2008) estimated SO₂ emission rates from the volcano using a scanning DOAS instrument located on the northern flank of the volcano. These emission rates were compared with estimates from a COSPEC instrument and from transects of an airborne DOAS aboard an ultra-light aircraft. Daily average values were in the range of 0.6 to 4.4 Gg/day, corresponding to 7 to 50 kg/s. These values are similar to measurements made in April 2003 during the MCMA-2003 field campaign, where two transects yielded estimates of around 0.8 Gg/day (10 kg/s) (de Foy et al., 2007) and to COSPEC estimates of 2 to 3 Gg/day (20 to 25 kg/s) during a pre-eruptive period leading up to August 1995, and 9 to 13 Gg/day (100 to 150 kg/s) during an effusive-explosive period from March 1996 to January 1998 (Delgado-Granados et al., 2001).

The Tula industrial complex is the home of a number of industries including a power plant and a refinery, and is located about 70 km northwest of the MCMA centre – diametrically opposite to the Popocatepetl volcano, see Fig. 1. The total official inventory for the area estimates SO₂ emissions of 323 ktonne/year, corresponding to 10 kg/s (Rivera et al., 2009). Mini-DOAS transects from 24 March to 17 April 2006 estimated average SO₂ fluxes of 155 ± 120 ktonne/year (4.9 ± 3.8 kg/s) for the refinery and the power plant together (Rivera et al., 2009). These values are in agreement with similar transects carried out during the

MCMA-2003 field campaign which estimated emissions of 145 ktonne/year (4.6 kg/s), (de Foy et al., 2007).

The 2006 official inventory estimated emissions of SO₂ in the MCMA to be around 5.7 ktonne/year from point sources and 3.2 ktonne/year from area sources, corresponding to 0.18 and 0.10 kg/s respectively (Secretaría del Medio Ambiente del Gobierno del Distrito Federal, 2008). As these are much smaller than the emissions from the volcano and the industrial complex, the plume from the point sources should be detectable above background rural and urban measurements.

SO₂ plumes from volcanos have been detected by satellite using the Global Ozone Monitoring Experiment (GOME) as well as the Scanning Imaging Absorption Spectrometer for Atmospheric Chartography (SCIAMACHY) confirming that the SO₂ plumes from the Popocatepetl are some of the largest on earth (Khokhar et al., 2005), (Loyola et al., 2008). The Ozone Monitoring Instrument (OMI) on NASA's Aura satellite provides higher spatial and spectral resolution combined with daily coverage providing retrievals of SO₂ column amounts (Krotkov et al., 2006). In addition to detecting volcano plumes (Yang et al., 2007), it has also been able to detect SO₂ plumes from copper smelters (Carn et al., 2007). Evaluation of the retrievals over Northeast China found that OMI could distinguish between background conditions and heavy pollution on a daily basis, with noise in the data of around 1.5 DU (Dobson Units), which can be reduced to 0.3 DU with spatial and temporal averaging (Krotkov et al., 2008). The algorithm has been further refined to improve retrievals of very large loadings from volcanic plume, and detected over 1000 DU from the Sierra Negra eruption in Ecuador in October 2005 (Yang et al., 2009). Given the emissions of the Tula industrial complex and the Popocatepetl, it should be possible to detect these under routine monitoring conditions.

1.2 Basin-scale wind transport

The MCMA is located in the subtropics where there is weak synoptic forcing and at high elevation surrounded by mountains leading to weak winds and complex flow patterns. Jau-regui (1988) describe the drainage flow into the basin that is decoupled from the westerlies aloft and accentuated by the urban heat island. At a time when SO₂ emissions were much larger in the city itself, this led to the highest SO₂ concentrations located at the centre of the heat island. Williams et al. (1995) simulated SO₂ dispersion in the MCMA and identified complex mixing suggesting that an elevated plume was entrapped in the drainage flow down Pico de Tres Padres and transported to the basin floor at night. Starting in 1992, the SO₂ content of fuels was reduced in the MCMA leading to a dramatic reduction of average concentrations from around 60 ppb to below 10 ppb currently (see Sistema de Monitoreo Atmosférico, <http://www.sma.df.gob.mx/simat2/informaciontecnica>). In terms of SO₂, this has shifted the concern from urban sources to regional point sources.

Particle trajectories were used by Bossert (1997) to show how an undercutting plain-to-plateau density current could transport pollutants into the basin with minimal mixing even though the urban plume was being vented aloft, moving above the surface current in the opposite direction. Fast and Zhong (1998) describe the recirculation patterns in the basin where the plume is transported along the surface, up the mountain slopes, and back over the urban area where it could mix back down to the surface, but was usually efficiently vented. A conceptual model of wind transport for the MCMA-2003 field campaign found stable drainage flows on most nights, accompanied by weak, stable winds from the north. These met with a gap flow from the southeast to cause a convergence line and rapid venting of the urban plume (de Foy et al., 2006c). The location and movement of these convergence lines determined the location of high pollution events in the basin (Jazcilevich et al., 2005), (de Foy et al., 2006a). These studies suggest that both the Tula plume below the basin and the Popocatepetl plume above could have significant impacts in the MCMA.

1.3 Sulfur transport

Episodes of high SO₂ concentrations and sulfate aerosol loadings were measured in the south of the MCMA in November 1997 and were attributed to emissions from Popocatepetl based on estimates of emission rates and dilution due to vertical mixing (Raga et al., 1999). These findings were corroborated by measurements during 2001 which identified high sulfate formation at southwestern measurement sites in the basin during moist periods from April to June when the volcano was active (Moya et al., 2003). In contrast, aerosol measurements during the IMADA field campaign were compared at boundary and urban sites, suggesting that transport from north to south accounted for about

two-thirds of the sulfate in the MCMA (Chow et al., 2002), and that these might be from the Tula industrial complex.

During the MCMA-2003 field campaign (Molina et al., 2007), aerosol measurements found high particulate sulfate loadings associated with transport from the north (Salcedo et al., 2006). Concentration field analysis of SO₂ time series data suggested that the Tula industrial complex accounted for the high SO₂ episodes during the campaign (de Foy et al., 2007). Forward Eulerian modelling of Popocatepetl emissions suggested that there could be urban impacts, but that these could not be differentiated from local emissions during April 2003.

With prevailing winds during the dry season from the west, the Popocatepetl plume would be more likely to be transported to the east past Puebla. It was detected there during a field campaign in April and May 1999 (Jimenez et al., 2004). Measurements of ozone and carbon monoxide were used to distinguish between urban and volcanic air masses, showing increases in sulfate aerosols due to the volcano. Juarez et al. (2005) found air quality impacts in the city of Puebla itself during an intense volcanic activity between December 2000 and January 2001. Measurements at the end of February 2001 in Pico de Orizaba National Park, over 200 km to the east, were carried out to determine the air quality impacts of neighbouring cities (Marquez et al., 2005). Pyle and Mather (2005) point out that in addition to urban impacts, the measurements indicated impacts of both SO₂ and sulfate aerosols from Popocatepetl. While these studies are focused on longer range transport, they do show that the plume can have surface impacts through downmixing, and that consequently with winds aloft to the west, Popocatepetl should significantly influence MCMA's air quality. Furthermore, the large variability in emissions opens up the possibility of very large MCMA impacts during episodes with particularly large emissions.

1.4 Outline

The synoptic meteorological conditions and meteorological measurements available during MILAGRO are described in Fast et al. (2007). The basin scale conditions were shown to be climatologically representative of the warm dry seasons of the last 10 years (de Foy et al., 2008). Cluster analysis was used to identify both surface wind features and vertical stratification of wind layers, leading to a conceptual model of the basin transport with six main categories (de Foy et al., 2008) which were similar to those of MCMA-2003 (de Foy et al., 2005). Overall, the analysis shows that there were days with venting both to the south and to the north, with complex mixing and stratification in the vertical.

So as to identify the sources of individual plumes in the basin, we carry out detailed analysis of ground measurements of SO₂ concentrations in combination with hourly maps of surface winds and daily evolution of vertical profiler winds. Column measurements from satellite remote

sensing provide a spatial view of the plume dispersion. Model comparisons are then used to integrate the different measurements available and to evaluate basin dynamics and plume impacts. At the same time, the measurements provide constraints on model performance and identify both model weaknesses and sources of uncertainty. This paper will describe specific episodes, but the entire set of surface wind vectors and radar wind profiler data is shown in the supplementary material <http://www.atmos-chem-phys.net/9/9599/2009/acp-9-9599-2009-supplement.pdf> for readers who desire extra supporting evidence or who are interested in other episodes.

2 Measurements

Figure 1 shows the location of the measurement sites used in this study. The Ambient Air Monitoring Network (Red Automática de Monitoreo Atmosférico, RAMA) operates a network of surface stations measuring meteorological parameters and criteria pollutants throughout the city. Quality-assured data at 1-hour intervals was used for the statistical comparisons and the hourly plots. This was available for the full month of March from 19 stations. Data at one-minute intervals was used for the plume time series plots to show the detailed transport in the basin. Wind vectors were available from 14 stations during the campaign.

SO₂ measurements were made using pulsed UV fluorescence (Teledyne API models 100 and 100A). UV radiation of 214 nm is passed through the sample chamber. UV photons are absorbed by SO₂ molecules which return to their ground state by emitting a lower energy photon with a wavelength of 330 nm. When the temperature is known, the amount of fluorescent light is directly related to the SO₂ concentration in the sample chamber. The measurements were digitised with 1 ppb increments, and had a stated instrument accuracy of 1% but likely overall measurement accuracy within 10%.

Two mobile laboratories were deployed with similar equipment, one at Santa Ana Tlacotenco (SATL), a small village on the southeastern edge of the basin overlooking the MCMA, and one at Tenango del Aire (TEAI), in the mountain pass to the southeast below the Popocatepetl volcano. The Aerodyne mobile laboratory (Kolb et al., 2004) was located at the summit of Pico de Tres Padres (PTP) from 8 to 19 March. SO₂ data were available starting on 13 March. This site is approximately 750 m above the basin floor in the north of the MCMA. It therefore serves as a background site at night, observes the mixing of the morning emissions during the day and the outflow of the urban area on afternoons with strong gap flows from the southeast.

At PTP and at T1, SO₂ was measured with a Thermo 43C pulsed fluorescence instrument which was periodically calibrated by standard addition. The background signal of the instrument was periodically measured with a Na₂CO₃ impregnated filter. The detection limit was of the order of 50 pptv

for a one minute average. Owing to less frequent SO₂ calibration while at PTP, the overall PTP measurement accuracy is likely below 20%.

A detailed description of the meteorological data collected during the campaign can be found in Fast et al. (2007) and in de Foy et al. (2008). In addition to the RAMA, SATL and TEAI wind vectors, this study uses winds from the five surface stations of the Mexican National Weather Service (SMN) located in the basin, as well as meteorological measurements from temporary stations at the T0, T1 and T2 sites.

Radar wind profilers were installed at T0, T1 and T2. These were 915 MHz models manufactured by Vaisala. They were operated in a 5-beam mode with nominal 192-m range gates. As described in Doran et al. (2007), the NCAR Improved Moment Algorithm was used to obtain 30-min average consensus winds. Plots of horizontal winds aloft also show the radiosonde observations from the SMN headquarters (GSMN) launched every 6 h. The timezone in the MCMA was Central Standard Time (CST = UTC−6) during the entire campaign, all times reported in this study will be in CST.

The Ozone Monitoring Instrument (OMI) provides SO₂ retrievals with a nadir resolution of 13 by 24 km and daily overpasses of the MCMA between 12:00 and 14:00. This study uses the level 2, version 3 swath data available online from NASA's Goddard Earth Sciences Data and Information Services Center. The total planetary boundary layer SO₂ column product was used (Krotkov et al., 2006), as we were interested in the urban impacts in the MCMA.

3 Modelling

Mesoscale meteorological simulations were carried out with the Weather Research and Forecast model version 3.0.1 (WRF, Skamarock et al., 2005) using the Global Forecast System (GFS) as initial and boundary conditions. There were three domains in the simulation with grid resolutions of 27, 9 and 3 km, 41 vertical levels and one-way nesting. Diffusion in coordinate space was used for domains 1 and 2, and in physical space for domain 3 (Zängl et al., 2004). The following options were used: the YSU boundary layer scheme (Hong et al., 2006), the Kain-Fritsch convective parameterisation (Kain, 2004), the WSM6 microphysics scheme, the Dudhia shortwave scheme and the RRTM longwave scheme. High resolution satellite remote sensing was used to improve the land surface representation in the NOAA land surface model for domains 2 and 3 by using landuse, surface albedo, vegetation fraction and land surface temperature from the Moderate Resolution Imaging Spectroradiometer (MODIS) as described in de Foy et al. (2006b).

The full details of the simulations and their evaluation are presented in de Foy et al. (2009). This compared the results of the simulations used in this study ("WRFb") with an alternative set-up of WRF ("WRFa") and with results from MM5.

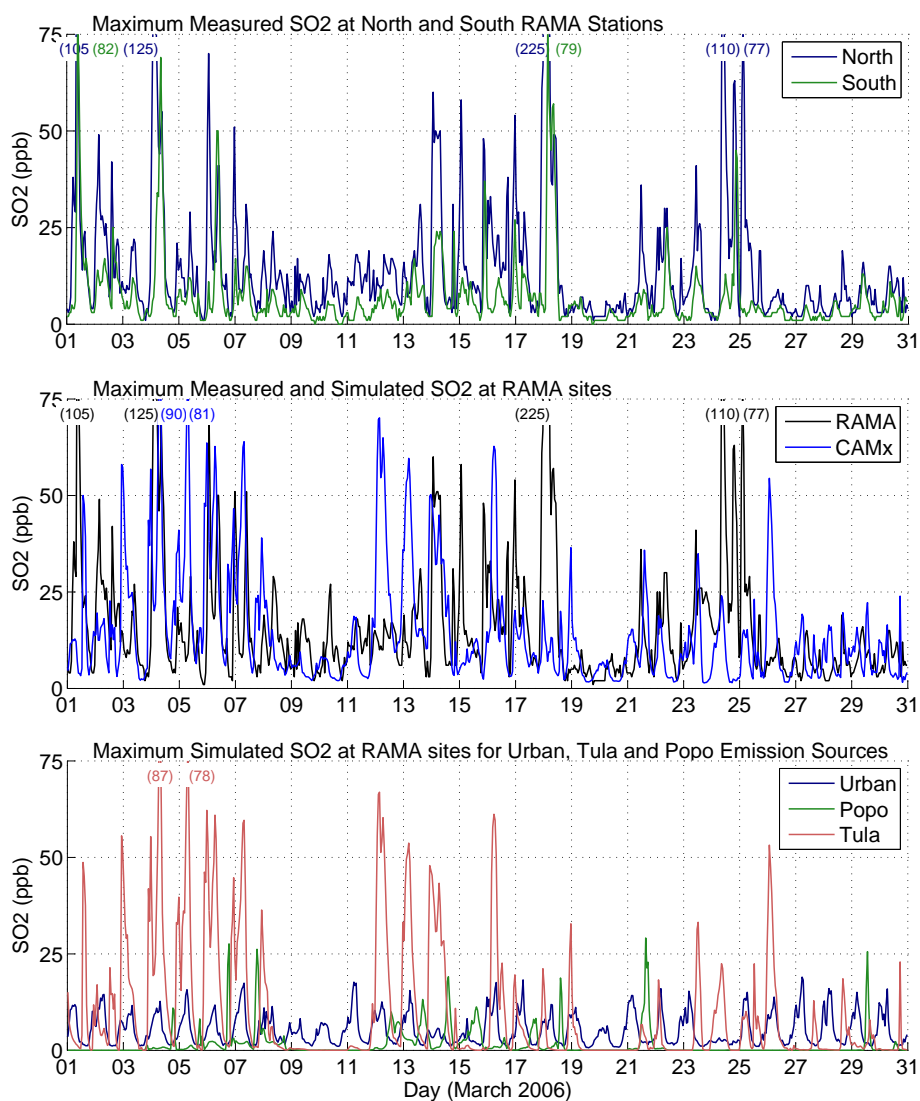


Fig. 2. Measured and simulated SO₂ in the MCMA. Maximum 1-hour concentrations for the North and South station groups defined in Fig. 1 (Top). Comparison of maximum domain-wide RAMA measurements and CAMx simulations (Middle). Domain-wide maximum of CAMx simulations for all RAMA stations measuring SO₂, for separate source groups (Bottom). Maximum of values off the chart shown in brackets.

By analysing wind roses segregated by clusters, it was shown that the drainage flows in the basin were under-represented in the model. It was further shown that the model had too much vertical stratification of winds. Nevertheless, by evaluating the model against transport of carbon monoxide and SO₂, it was shown that the simulations were a representative approximation of actual transport in the basin. On the basis of this, it was suggested that following Oreskes (1998), the simulations met the criteria for “Aristotelian Accuracy” by being of sufficient quality for the purposes at hand (de Foy et al., 2009).

Eulerian pollutant transport was calculated using the Comprehensive Air-quality Model with eXtensions (CAMx, ENVIRON (2008)), version 4.51. This was run on the finest

WRF domain at 3 km resolution with the first 18 of the 41 vertical levels used in WRF, corresponding to approximately 6000 m above ground level. Chemistry was turned off and the simulation was carried out for SO₂ acting as a passive tracer. The vertical diffusion coefficients of O’Brien (1970) were modified using the kvpatch processor to reset the minimum in the bottom 500 m layer to 1 m²/s over urban areas and 0.5 m²/s over forests. Boundary and initial conditions for SO₂ were set to 1 ppb based on GOME satellite retrievals available at the Belgian Institute for Space Aeronomy (IASB-BIRA). More details and an evaluation of the model setup is presented for the MCMA-2003 field campaign in de Foy et al. (2007).

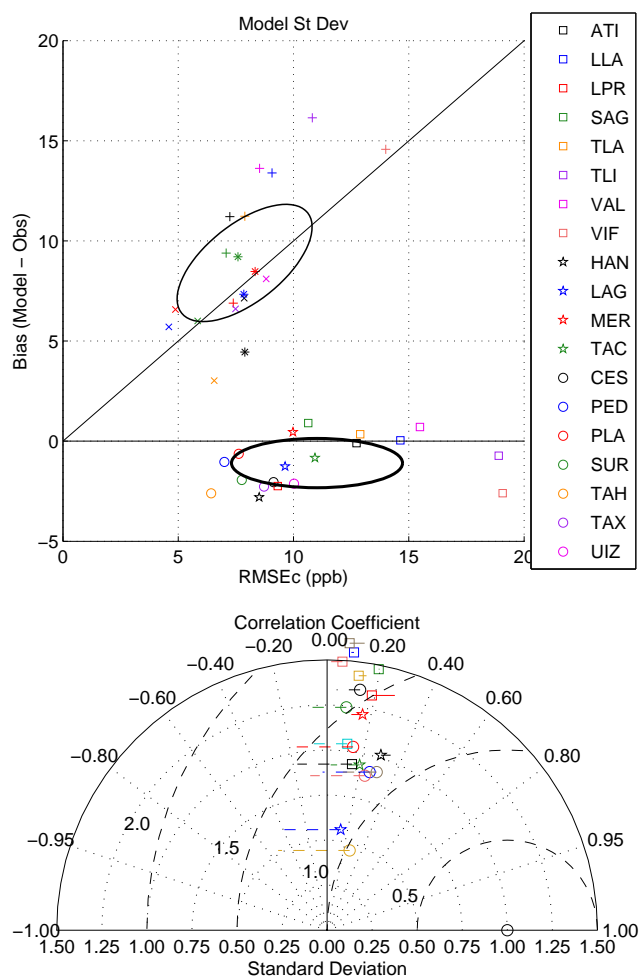


Fig. 3. Statistics diagrams of simulated versus measured hourly SO₂ by station in the MCMA. Top: RMSEc-bias diagram, open symbols show the model bias versus the centred root mean square error (RMSEc). Closed symbols show the model standard deviation versus that of the observations (squares match '+', circles match 'x'). Ellipses are centred on the mean with semi-axes given by the standard deviations of the metrics. Bottom: Taylor diagram showing the correlation coefficient and the standard deviation, solid horizontal line indicates positive bias, dashed line for negative bias.

The emissions for the Tula industrial complex were taken from Rivera et al. (2009) and those for the Popocatepetl were interpolated on an hourly basis from the daily values reported in Grutter et al. (2008). For the Popocatepetl volcano, the maximum terrain height in the model is 4438 m m.s.l.. The emissions were therefore released at a height of 1027 m above ground, to correspond to the actual summit of the mountain at 5465 m m.s.l. MCMA urban emissions were much lower than these point sources and were based on the 2006 official emissions inventory for the MCMA (Comisión Ambiental Metropolitana, 2008).

4 Results

Figure 2a shows the maximum hourly SO₂ concentrations measured by RAMA stations in the north and south of the MCMA during the whole MILAGRO campaign. The stations used for each group are shown in Fig. 1. We show the maximum concentrations by domain because we are interested in looking at the sources of large plumes. Baseline levels are low, with a clear diurnal cycle starting at 5 ppb at night and rising to 20 ppb during the day. The main feature in the time series are the short spikes in concentrations at night rising up to a campaign maximum of 225 ppb. Concentrations are clearly higher in the north of the MCMA. The baseline levels in the south vary from 0 to 5 ppb, and the spikes rarely reach the same levels as those of the northern domain.

The comparison between measured and simulated maximum domainwide concentrations is shown in Fig. 2b. Qualitatively, this is in agreement with the measurements in terms of both the base line levels and the presence of high concentration episodes. Three time periods exhibit relatively high numbers of SO₂ spikes: the South-Venting flow of the early campaign (1–8 March), the days following the Cold Surge events on 14 March and again after 21 March. Figure 3 shows the statistical metrics for the hourly time series by station using the Taylor diagram (Taylor, 2001) and RMSEc-bias diagram (de Foy et al., 2006b). Overall, the simulated maximum SO₂ levels are too low by 1.8 ppb, the centred Root Mean Square Error is 24 ppb, Pearson's correlation coefficient is 0.14 and the Index of Agreement (Willmott, 1982) is 0.39. For the domainwide mean, these values are 1.1 ppb too high, 8.4 ppb, 0.24 and 0.48 respectively. Figure 2b shows that these low performance indices are mainly due to false positives and false negatives. Case-by-case analysis below will show that this is because the point sources are 70 km from the urban centre, and that small differences in the wind fields can make the difference between the plumes missing or hitting the measurement sites, but that the model nevertheless represents the dominant flow features and transport directions in the basin.

Finally, Fig. 2c shows the maximum 1-h CAMx simulated concentration levels for all RAMA stations for three different sources: the urban sources, the Popocatepetl volcano and the Tula industrial complex. This suggests that urban sources are responsible for a small, regular, diurnal variation in SO₂, that the volcano causes occasional peaks in the model and that most of the high SO₂ peaks are due to transport from the Tula industrial complex.

4.1 OMI evaluation

Figures 4 and 5 show the total planetary boundary layer columns of SO₂ measured by the OMI sensor as well as columns simulated by CAMx for all sources (urban, Tula and Popocatepetl) for eight days during the campaign. These cases clearly show high SO₂ columns over the Popocatepetl

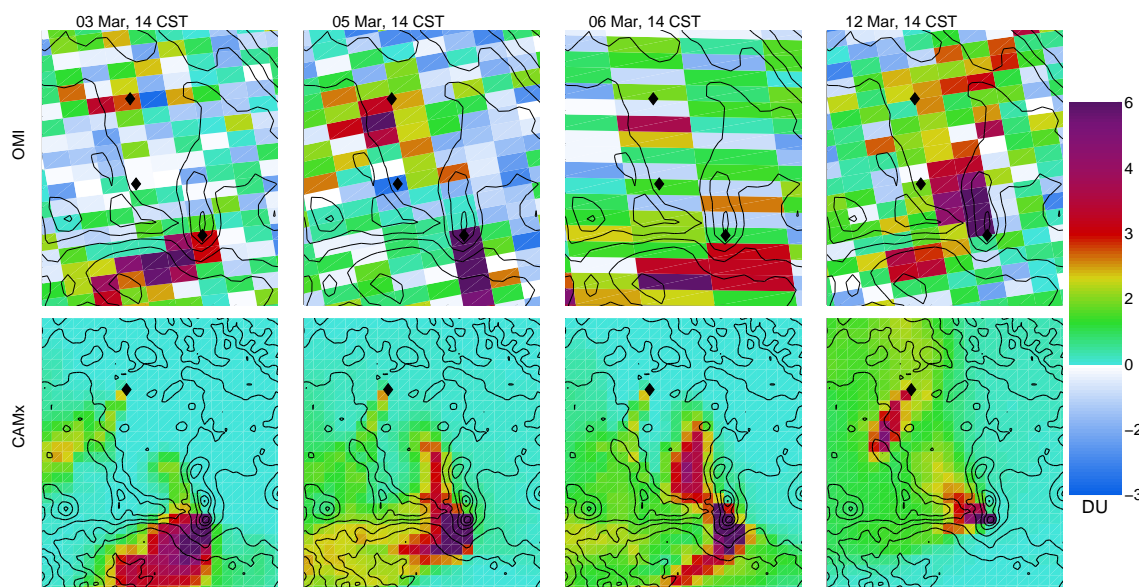


Fig. 4. SO₂ total columns from OMI swath data and CAMx regional simulations with 9 by 9 km grid cells with all sources (urban, Tula and Popocatepetl). Black diamonds shows the location of Tula and Popo. Terrain contours every 500 m.

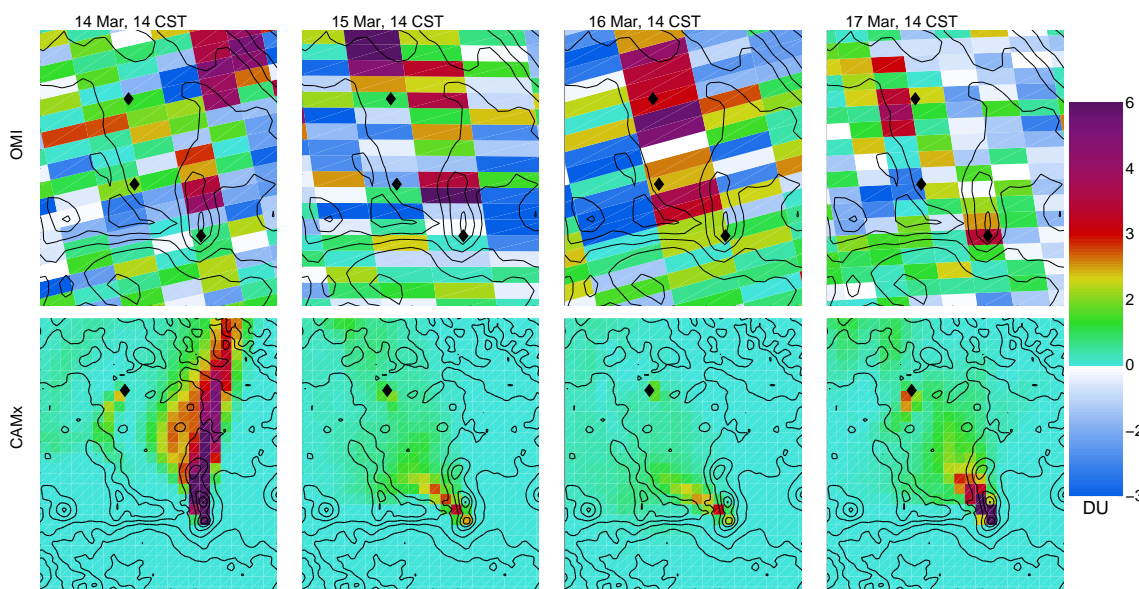


Fig. 5. SO₂ total columns from OMI swath data and CAMx regional simulations with 9 by 9 km grid cells with all sources (urban, Tula and Popocatepetl). Black diamonds shows the location of Tula and Popo. Terrain contours every 500 m.

volcano and over the Tula industrial complex. Both the direction and the intensity of each plume varies from day to day. The industrial plume rapidly dilutes to below detection level of the OMI sensor, but the volcano plume can be tracked for longer distances.

Figure 6 shows the monthly composite of all the swath data available mapped onto the CAMx grid, with the corresponding average model result. Based on the OMI user's guide (OMI Team, 2009), only swath pixels between cross

track positions 10 and 50 were used for which the radiative cloud fraction was less than or equal to 0.2. These swath pixels were projected onto a 3 by 3 km grid using nearest neighbour interpolation. A monthly average was created from the 29 available daily grids.

By oversampling the SO₂ data at a fine resolution, this image fusion method is able to provide an image of the average plume at a higher resolution than the original data. This is similar to the goal of super-resolution (Capel, 2004),

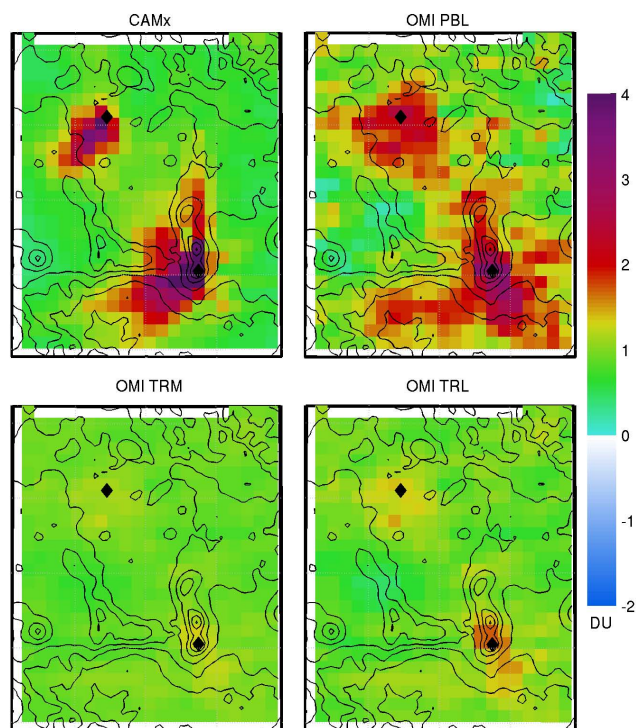


Fig. 6. Average SO₂ total columns for 3 to 31 March 2009 from OMI swath data and CAMx regional simulations with 9 by 9 km grid cells and all sources (urban, Tula and Popocatepetl). Black diamonds shows the location of Tula and Popo. Terrain contours every 500 m.

which has been successfully applied to land cover mapping (Li et al., 2009), (Boucher et al., 2008). Super-resolution works because the underlying map can be assumed to be constant. In the present case however the SO₂ plumes are always changing and consequently the more sophisticated methods cannot be directly applied.

The background SO₂ concentration of 1 ppb in the simulations leads to a vertical column of 0.4 DU. The OMI retrievals use a sliding median residual correction method to remove the along- and cross-track biases (Yang et al., 2007). Because of the high values in the MCMA region, this leads to a background of -0.5 DU. In order to account for this, we have added an offset of 0.9 DU to the satellite retrievals.

The values of the OMI retrieved PBL columns depend on the estimation of the air mass factor (AMF) defined as the ratio of the satellite measured slant column amount to the vertical column amount (Krotkov et al., 2008). Using basin averaged pressure and elevated vertical profiles of the Tula plume and a surface albedo value of 0.02 at 315 nm (Corr et al., 2009) increases the AMF by 10% compared to the operational AMF, which would reduce the PBL columns accordingly. Accounting for aerosols in the boundary layer using AERONET measurements and a single scattering albedo of 0.8 at 315 nm (Corr et al., 2009) decreases the AMF by

Table 1. Basin averaged bias (OMI minus model), centred Root Mean Square Error and Pearson correlation coefficient comparing the OMI PBL, TRM and TRL retrievals with the CAMx simulation.

Metric	OMI PBL	OMI TRM	OMI TRL
Bias	0.18	-0.18	-0.16
RMSEc	0.63	0.78	0.74
Pearson r	0.66	0.57	0.58

10% bringing it back to the same value as that used by default in the derivation of the PBL product (AMF=0.36). No correction was therefore needed for the operational values due the local conditions in the MCMA.

The monthly averages were spatially averaged to the same 9 by 9 km grid as the CAMx simulation for visual comparison. Model monthly averages were created by using simulation data at each grid point for which a corresponding OMI pixel was available. Statistical metrics were calculated between the simulated grids and the satellite retrievals by further aggregating the grid points to 18 by 18 km to account for the fact that the highest OMI pixel resolution is 13 by 24 km. Table 1 shows the basin averaged bias (OMI minus model), centred Root Mean Square Error and Pearson correlation coefficient between the OMI retrievals and the CAMx simulations (negative bias means the satellite retrievals were lower than the simulated columns).

This shows that OMI clearly detected both the Popocatepetl and the Tula industrial complex plumes. The main difference is the higher resolution of the plume afforded by the simulations leading to higher column values in the vicinity of the sources. The transport directions of the plumes are in qualitative agreement, with the Tula plume transported to the southwest and the Popocatepetl plume transported either to the north or to the southwest. While the plumes are detected in all three satellite products, it is clear that the PBL retrieval is the one that is most sensitive to the plumes, and closest to the simulations.

Detailed results will be presented for the 2, 5 and 6 March which are part of the first group of days with strong winds to the south, and for the period from 12 until 18 March which cover the first Cold Surge episode. Areas of agreement and discrepancy between the measurements and the simulations will be used to evaluate the transport processes and model performance on an individual basis.

4.2 Industrial impacts

A straightforward case of plume transport took place on 2 March, which was a day with strong winds from the north – a “South-Venting” day. Figure 7 shows variable SO₂ levels during the first part of the day followed by a uniform increase starting at 14:00 in the north at TLI, impacting urban

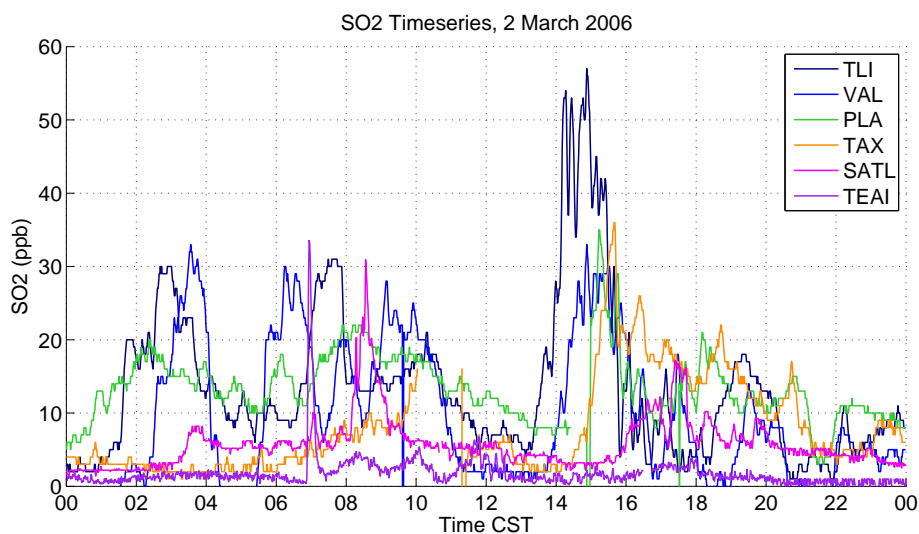


Fig. 7. Time series of measured SO₂ concentrations for 2 March.

sites at very similar times and SATL a little later. Figure 8 shows the transport to the south with a narrow plume extending through the centre of the MCMA. The combination of the surface wind vectors, the surface contours of SO₂ and the simulated plume provide strong evidence that the plume originated in Tula. Note that the plume extends from north to south, but moves from east to west in time as the wind direction changes very slightly. This illustrates how sensitive impacts are to small changes in the winds. Furthermore, in this case, the timing of the impact reflects the lateral movement of the plume rather than the speed of transport across the basin.

Figure 9 shows the time series of SO₂ concentrations for 5 and 6 March. Meteorologically, these are South-Venting days similar to 2 March. On the 5 March, levels remain low, but there is a well defined plume over the urban area from 08:00 to 12:00 and a second shorter one from 15:00 to 17:00. Surface winds and simulated contour plots, shown in Fig. 8, suggest that these are transport events from Tula.

On 6 March, the two plumes are much more clearly defined with levels reaching 70 ppb. Measured impacts are to the west of Pico de Tres Padres from 00:00 to 04:00. In the simulations, the drainage flows from the southwest basin rim are weaker and there is stronger wind from the northwest. This transports the plume just to the other side of PTP. With time, the plume moves towards the east outside of the urban area, and then returns at 08:00, with a clear and direct impact at Tenango del Aire. This is too early in the day to be downmixing from the volcano. Furthermore, the progression along the east side of the basin is well captured in the time series data. Note that the simulations capture both the westward transport at the surface, and the southward flow through the mountain gap in the southeast.

The OMI columns show clear transport of both the Tula and the Popocatepetl plume to the south for the 3, 5 and 6 March. Simulations are in agreement, with clearly a lot more SO₂ being emitted by the volcano than by the industrial complex. It would seem that there is insufficient SO₂ in the simulations for these days, although it is difficult to draw hard conclusions given the resolution of the features. Note however that part of the simulated volcano plume is entrained in the gap flow that forms northwards in the early afternoon. There is no evidence of this in the data, and setting a higher plume release height eliminates this feature entirely.

The episode from the 21 to 27 March shows similar transport of the Tula plume into the MCMA, albeit with more complex flows due to the weaker, moister winds causing afternoon convection. The simulated volcano spike on 21 March is most likely a false positive due to entrainment in an overly developed gap flow. The reader interested in individual episodes is referred to the supplementary material <http://www.atmos-chem-phys.net/9/9599/2009/acp-9-9599-2009-supplement.pdf> which shows hour by hour surface vectors and daily maps of radar wind profiler data.

4.3 Volcano impacts

SO₂ concentrations were low on 12 March, which had weak drainage flows into the basin followed by northerly surface flows and then a strong gap flow from the south in the late afternoon (“O3-South”). Figure 10 shows low levels of SO₂ throughout the day, but a distinct plume signature at Santa Ana (SATL) starting at 04:00 in the morning. There are short impacts at T1 around 06:00 followed by a uniform increase at sunrise at both Tenango del Aire (TEAI) and T1 which are at either end of the basin.

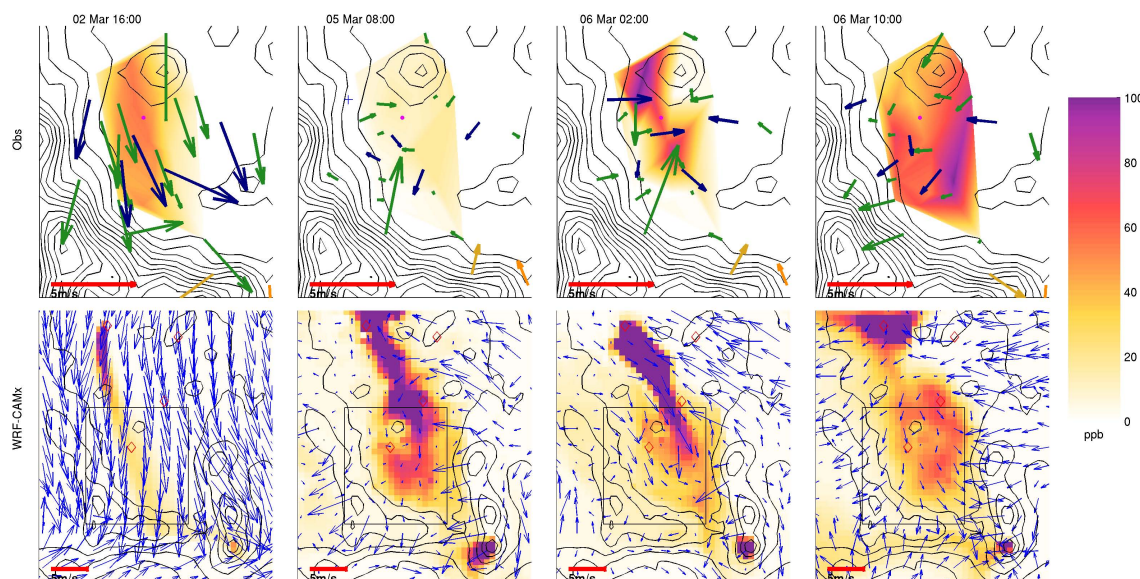


Fig. 8. Measured winds and hourly surface concentration of SO₂ in the MCMA and simulated winds (WRF) and SO₂ (CAMx, all sources) in the basin. Observed winds are coloured according to network: green - RAMA, blue - SMN, magenta - T1, tan - St. Ana, orange - Tenango del Aire. Terrain contours every 100 m (top) and 500 m (bottom), measurement domain shown as a box in model domain, red diamonds show T0, T1, T2 and Tula.

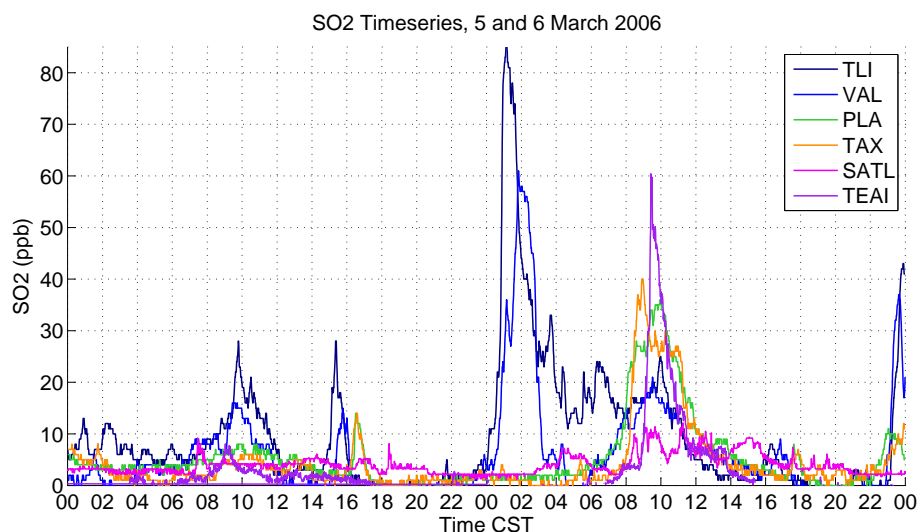


Fig. 9. Time series of measured SO₂ concentrations for 5 and 6 March.

The OMI columns in Fig. 4, show very clearly a split in the volcano plume. Part of it is transported towards the southwest, while the bulk of it is transported northwards where it covers the eastern side of the MCMA. This is represented by the model, albeit with lower total columns of SO₂. The Tula plume is simulated to move southwest, but was not detected by OMI.

Wind vectors show the strong drainage flow in the basin, see Fig. 11. The simulations do not represent this feature, and the gap flow moving northwards is stronger in the model

than the data suggests. Because of the combination of strong drainage flow and northeasterly flow in the north of the basin, the Tula plume that is simulated to reach the MCMA does not in fact enter the basin.

Instead, we suggest that the SO₂ on this day is from the volcano plume, with an initial impact at Santa Ana and some of the stations in the centre of the basin. The impacts at T1 at 06:00 correspond to an outburst of surface winds from the south in the radar wind profiler data (see supplementary material <http://www.atmos-chem-phys.net/9/9599/>

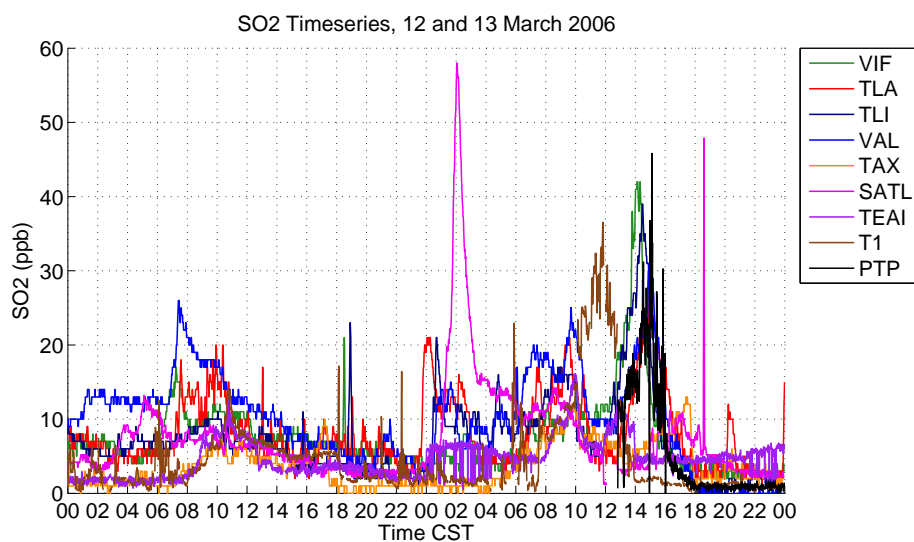


Fig. 10. Time series of measured SO₂ concentrations for 12 and 13 March.

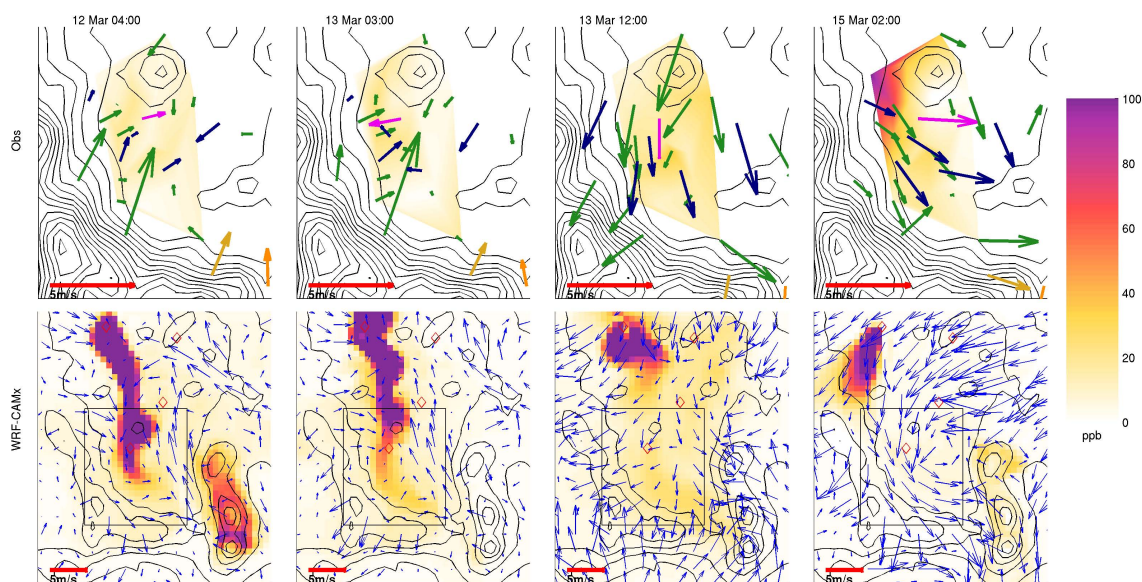


Fig. 11. Measured winds and hourly surface concentration of SO₂ in the MCMA and simulated winds (WRF) and SO₂ (CAMx, all sources) in the basin. Observed winds are coloured according to network: green - RAMA, blue - SMN, magenta - T1, tan - St. Ana, orange - Tenango del Aire. Terrain contours every 100 m (top) and 500 m (bottom), measurement domain shown as a box in model domain, red diamonds show T0, T1, T2 and Tula.

2009/acp-9-9599-2009-supplement.pdf), and the levels rise uniformly after sunrise at stations very far apart suggesting the presence of a wide, uniform plume aloft. A concentration of 10 ppb over a 4000 m boundary layer would correspond to a total SO₂ column of around 2 DU, which is in agreement with the OMI retrievals.

On March 13, there is a sharp plume at Santa Ana (SATL) at 02:00 in the morning. This occurs during strong drainage flows from the south at SATL. Levels of SO₂ rise across the basin suggesting a volcanic impact, although the excess SO₂

above 20 ppb could be due to a local source. Vertical stratification of the plume probably prevented impacts at the stations on the basin floor as well as at Tenango del Aire. Later in the day, there are strong winds from the north providing clear evidence of a Tula impact. This is the first day with SO₂ data at PTP. Concentrations similar to those at the basin floor show that the plume is well mixed within the boundary layer. SO₂ concentrations everywhere drop after sunset as the winds aloft start coming from the east and then from the south.

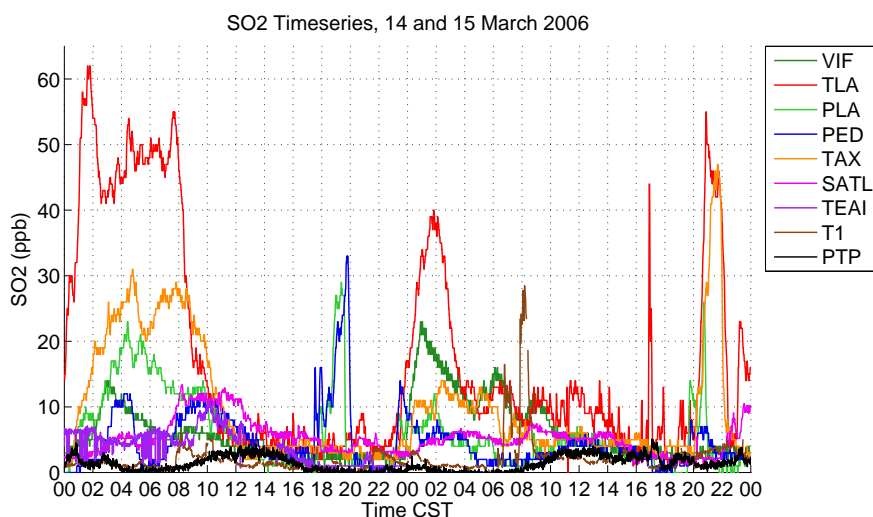


Fig. 12. Time series of measured SO₂ concentrations for 14 and 15 March.

4.4 Industrial surface impacts with volcano plume aloft

OMI retrievals for the 14, 15 and 16 March show clear transport of the volcano plume towards the north around midday, see Fig. 5. On the 14 there is a weak signal from Tula, possibly towards the south, but on the 15 it seems to move north with the Popocatepetl plume. Cold Surge events are associated with strong, cold surface winds from the north under the prevailing winds aloft, with strong vertical stratification of the flow. On 14 March, this is clearly reflected in a Tula plume from 00:00 to 10:00 that impacts the northwestern stations, see Fig. 12. It moves southwards through the whole western edge of the MCMA, reaching Santa Ana at 08:00 and Tenango del Aire at 09:00. The extent of plume dilution can be seen before sunrise as the plume moves south. Levels at PTP remain near zero however indicating that low vertical dispersion keeps the plume below the height of the stations (750 m above the basin floor). After sunrise, vertical dispersion rapidly dilutes the plume everywhere. From 18:00 to 20:00, there is a short impact as a plume skims the western edge of the basin. Wind vectors indicate that this is due to direct transport from Tula, similar to the situation on 2 March. Overall therefore, the Popocatepetl plume was not detected at the surface – although it might have impacted the eastern side of the basin.

On 15 March, transport is slightly more to the northwest suggesting possible volcano impacts over the city. The time series show a clear Tula plume starting at midnight, moving south into the basin without impacting PTP aloft, and then diluting during the day, see Figs. 11 and 12. There is a second Tula impact at 20:00 that is similar in structure. In between, there is no surface evidence of a Popocatepetl impact that would be significantly above the background levels. In particular, PTP does not register any SO₂ that cannot be readily attributed to local transport from vertical mixing.

On 16 March, SO₂ plumes impact mainly the north of the MCMA, see Fig. 13. The OMI retrievals show the volcano plume moving northwest over the basin and there are high columns both to the north and to the south of Tula. This would seem to be a perfect day for Popocatepetl impacts at the surface, but the radar wind profilers show a very strongly decoupled flow with a surface layer moving south and a layer above the boundary layer moving north, see Fig. 14. The high SO₂ is therefore clearly from Tula, moving around during the day with variable impacts. The pattern in the OMI retrievals around Tula is most likely due to the superposition of the two plumes, with the Tula plume moving south and the Popocatepetl plume moving north.

There is a convergence line in the north of the city which is accompanied by rapid increase and decrease in SO₂ concentrations including at PTP from 16:00 to 18:00. Later in the evening, at 21:00, there is a short lived spike at PTP as the plume moves over the north of the MCMA. This seems like a meteorological curiosity, where the edge of the plume was transported briefly over the mountain as it moved west but the bulk of the plume behind has gone around because of the nighttime stability, leaving low SO₂ conditions at PTP. The same feature was observed at 23:00 and then again at 05:00 the following day.

Conditions on 17 March are very similar to the previous two days, with the radar wind profilers showing winds from the north at the surface and from the south aloft, see Fig. 16. From 19:00 to 20:00, there is uniform flow from the south, and this coincides with the lowest levels of SO₂ of the day, further indicating that Tula, rather than Popocatepetl, is the source of the SO₂.

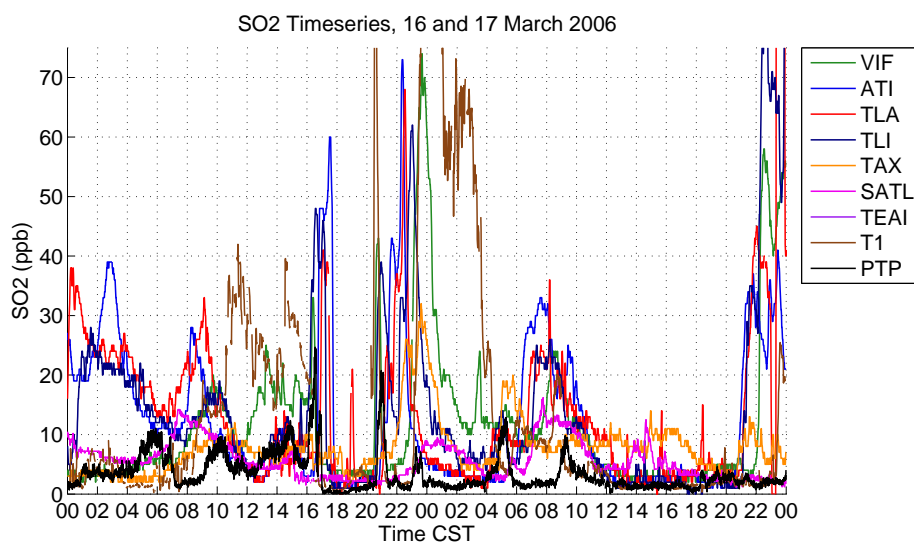


Fig. 13. Time series of measured SO₂ concentrations for 16 and 17 March.

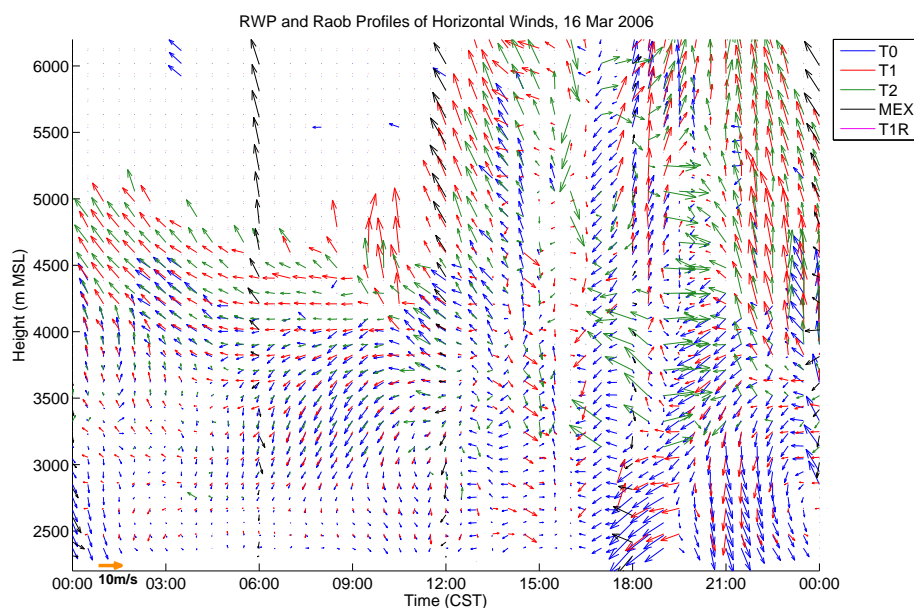


Fig. 14. Radar wind profiler and Radiosonde wind vectors at GSMN, T0, T1 and T2 on 16 March 2006. This shows the evolution of horizontal winds with height, an arrow pointing up means winds moving north. MEX are the radiosondes launched at GSMN, T1R are the radiosondes launched at T1.

4.5 Double impacts

Following a couple of hours of clean southerly air on 17 March, there is a northerly surface layer that brings with it the Tula plume and the highest SO₂ levels of the campaign on 18 March. Levels drop to around 50 ppb during the morning and by 14:00, strong winds from the south have cleaned the basin. Combined with the impact of a holiday week-end, this now sets the stage for the cleanest day of the campaign on 19 March. Unfortunately, the plumes cannot be seen in

the OMI retrievals for the 18 March because the MCMA is on the edge of the swath.

Figure 17 shows the time series at selected stations. One minute concentrations reach above 200 ppb at a number of stations before sunrise. At PTP, levels rise to 10 ppb at 01:30 and remain at this level until they increase to 70 ppb from 05:30 to 07:00. By this time, the levels have dropped at the stations below, and it is only after sunrise that the surface concentrations rise again to values between 30 and 50 ppb. There is a sudden spike at T1 from 09:00 to 10:00 after which

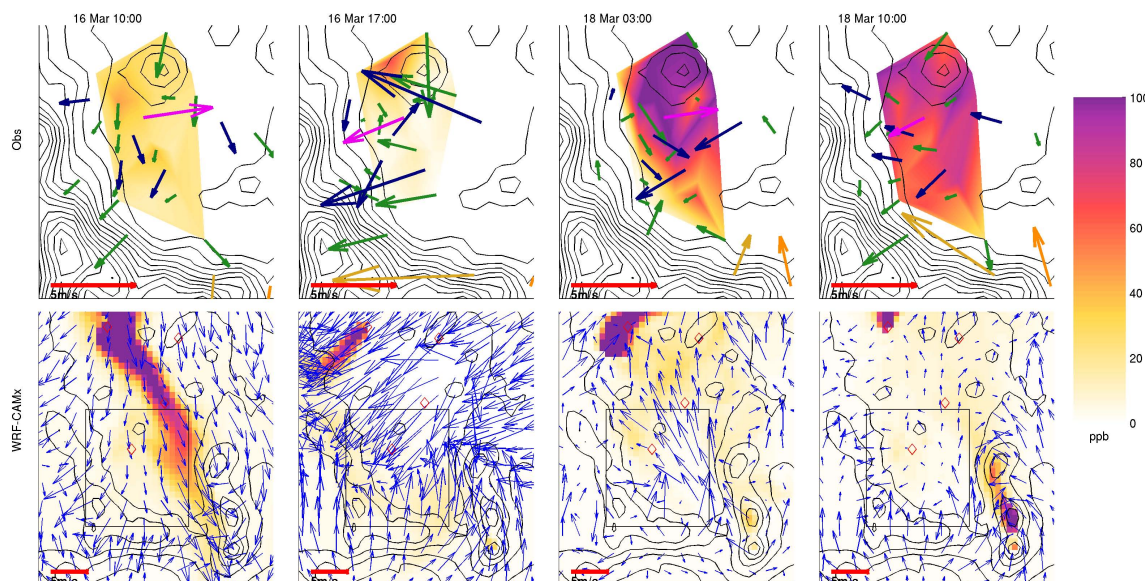


Fig. 15. Measured winds and hourly surface concentration of SO₂ in the MCMA and simulated winds (WRF) and SO₂ (CAMx, all sources) in the basin. Observed winds are coloured according to network: green - RAMA, blue - SMN, magenta - T1, tan - St. Ana, orange - Tenango del Aire. Terrain contours every 100 m (top) and 500 m (bottom), measurement domain shown as a box in model domain, red diamonds show T0, T1, T2 and Tula.

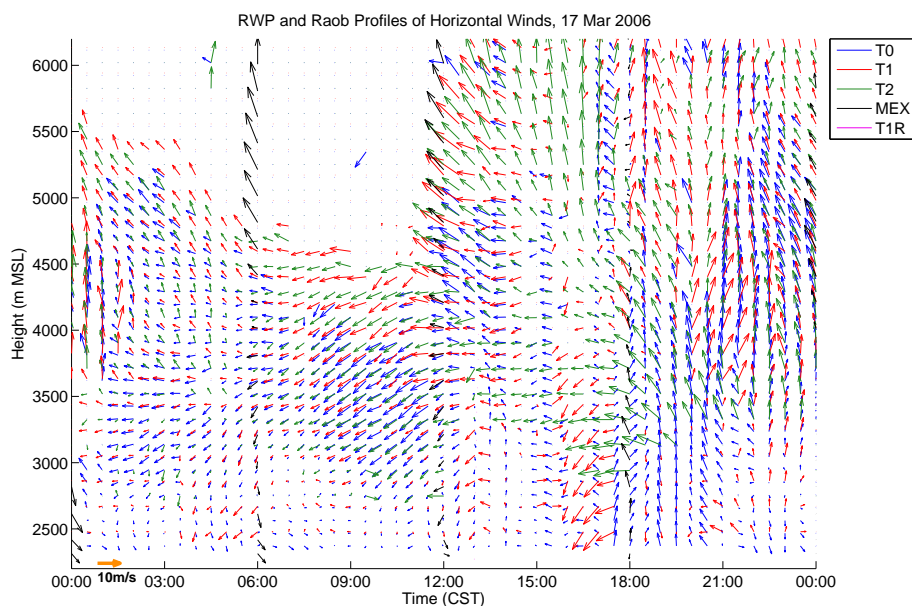


Fig. 16. Radar wind profiler and Radiosonde wind vectors at GSMN, T0, T1 and T2 on 17 March 2006. This shows the evolution of horizontal winds with height, an arrow pointing up means winds moving north. MEX are the radiosondes launched at GSMN, T1R are the radiosondes launched at T1.

the concentrations return to similar values as other northern sites, and then shortly before 12:00 the concentrations drop to under 10 ppb.

The surface wind vectors provide a clear picture of transport from Tula around PTP, see Fig. 15. There is a strong gap flow indicated by southerly winds at the eastern stations.

The radar wind profiler data clearly show a layer 500 m thick or less that is from the northwest, with strong southerly flow aloft, see Fig. 18. By 04:00, the southerly flow at T0 has caused SO₂ concentrations to drop, but now there are higher concentrations at TAX in the south. At PTP, the concentrations rose at 01:30 when the winds started to come from the

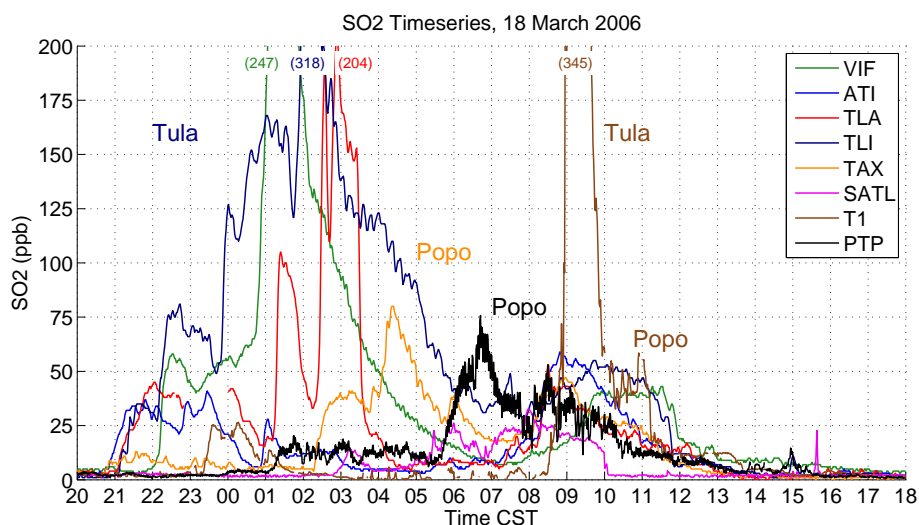


Fig. 17. Time series of measured SO₂ concentrations for 18 March. Maximum of values off the chart shown in brackets. Tula and Popo plumes labelled with the colour of the corresponding site.

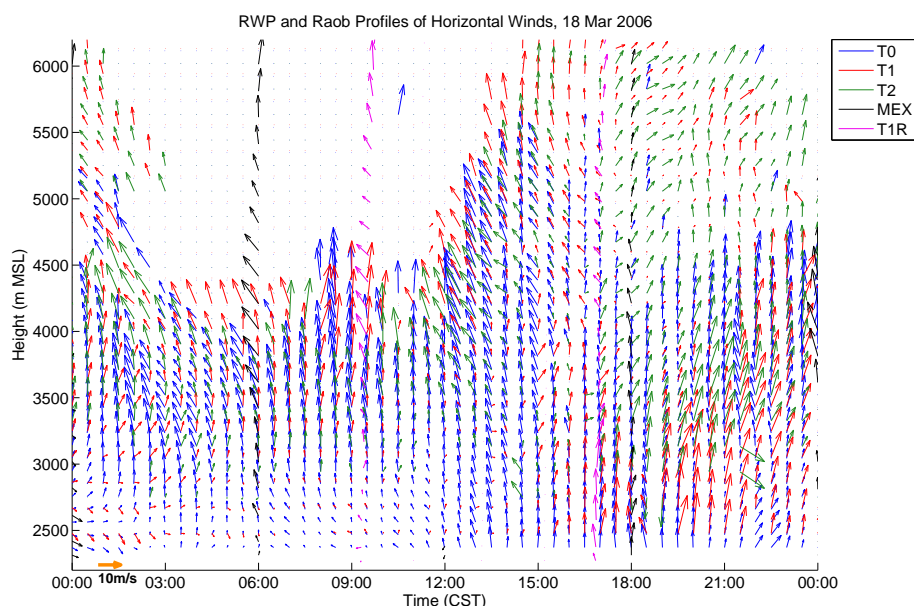


Fig. 18. Radar wind profiler and Radiosonde wind vectors at GSMN, T0, T1 and T2 on 18 March 2006. This shows the evolution of horizontal winds with height, an arrow pointing up means winds moving north. MEX are the radiosondes launched at GSMN, T1R are the radiosondes launched at T1.

southsoutheast at 3000 m.s.l. The increase around 06:00 coincides with winds turning slightly to be more from the direction of the volcano. The concentrations are now higher aloft than anywhere at the surface, and it is only after sunrise, with the start of vertical mixing, that concentrations rise to levels comparable to those at PTP. At T1, the shallow northerly layer lasts longer and includes a brief period of westerly winds that brings high concentrations from 09:00 to 10:00 before the concentrations subsequently return to levels comparable to the other northern stations. Fig. 15 shows

strong surface wind vectors from the east at 10:00 with a strong gap flow from Tenango del Aire.

Combining the evidence, one can see that the day starts with a Tula plume at the surface. Concentrations are higher than usual because the surface layer is shallower than normal, suppressing vertical dispersion. Meanwhile, the volcano plume is transported over the basin, causing impacts at PTP starting at 01:30, at TAX after 02:00 and at SATL after 03:00. The impacts subsequently increase first at TAX, then at PTP. After sunrise vertical mixing starts and the plume

is mixed down to the surface at the northern stations. By 12:00, the winds now blow due north and the volcano plume no longer impacts the basin. The 09:00 spike at T1 must be of Tula origin, when one considers the surface layer flow in the radar wind profiler data, and the concentrations that are higher than any other station, especially PTP above it.

In terms of simulations, the early morning gap flow is over-represented, preventing the formation of a shallow northerly layer, sweeping the basin clean and causing the Tula plume to vent to the north. The easterly basin flows in the morning are under-represented, limiting the simulated Popocatepetl impacts to the eastern edge of the basin. This case provides a clear example of how the model tries to represent features of the basin flow, but discrepancies in the detailed representation lead to large differences in the industrial and the volcanic plume.

5 Conclusions

Detailed case by case analysis of the SO₂ plumes in the MCMA using both meteorological observations and numerical simulations suggest that most of the large peaks observed during MILAGRO originate in the Tula industrial complex. In comparison, the Popocatepetl volcano had smaller impacts on fewer occasions. Numerical models of plume dispersion were able to simulate impacts from both plumes. The analysis confirms past meteorological studies and illustrates the night-time flow into the basin from the north under stable conditions. Vertical mixing during the day was observed at PTP occurring from both the ground up, in the case of the industrial plume, and from the layer above down to the ground in the case of the volcano plume. 18 March in particular illustrates how complex wind patterns can be in the MCMA with the highest impacts of the campaign from both sources occurring in immediate succession. There were both false positives and negatives of simulated Tula impacts in the basin which were shown to result from small variations in wind direction. Subtle changes in the strength of the down-valley flow from Pachuca to the northeast, and the up-valley flow to Tula also from the northeast could totally change the resulting plume transport at Tula between going south towards the MCMA or being vented northwards. While this provides a cautionary tale in the evaluation of model output, it also shows that by interpreting the results using both data and models a reasonable degree of confidence can be reached.

Table 2 shows the percentage of the mean simulated SO₂ impacts in the MCMA due to the three different source groups in CAMx. This was calculated by summing SO₂ concentrations from CAMx simulations with individual source groups for every hour of the campaign. In this instance we are interested in mean values as way of identifying the relative importance of the emission inventories, but using the maxima (see Fig. 2c) yields the same results. For comparison, impact fractions are presented using the different

Table 2. Percentage of mean SO₂ concentrations in the MCMA due to each source group during March 2006. “WRFa” and “MM5” refer to simulations discussed in de Foy et al. (2009), Popocatepetl releases at 4438 m and 6438 m correspond to 0 and 2000 m release heights above the model surface, Tula no plume rise has releases set at stack height, which made a negligible difference.

Model Run	Urban	Popocatepetl	Tula Ind. Complex
WRF	37%	10%	53%
“WRFa”	46%	14%	40%
“MM5”	39%	5%	57%
Popo 4438 m release	34%	18%	48%
Popo 6438 m release	37%	3%	57%
Tula no plume rise	37%	10%	53%

simulations discussed in de Foy et al. (2009), as well as for different release heights for the Popocatepetl and the Tula industrial complex. As expected, the lower volcano release height leads to higher estimated impacts and conversely the higher release lowers the impacts. The Tula plume rise however makes no significant difference to the results, suggesting that the findings are robust with respect to estimates of plume parameters. Overall, about one tenth of the SO₂ in the MCMA during MILAGRO could be due to the volcano with the rest split between the Tula industrial complex and local urban sources. This finding is not significantly affected by model setup. This represents an increase over the 20% of impacts thought to be caused by Tula during MCMA-2003. Such variation can easily be caused by changes in wind patterns, with the higher numbers during MILAGRO due to the week of strong northerly flows at the beginning of March 2006. Furthermore, both of these episodes are during the warm dry season when the westerlies are the prevailing winds aloft. The numbers could change significantly during the wet season when the weak, easterly trade winds dominate aloft. Further analysis and modelling work would be needed to explore the impacts of more transport to the east and increased stratification in the basin due to weaker winds.

Satellite retrievals of total SO₂ columns from OMI were shown to detect both the industrial and the volcanic plumes, and were in broad agreement with simulations. The OMI data was of sufficiently high resolution to identify some of the features of the plume transport. Furthermore, oversampling the swath data to a fine grid (3 by 3 km) and averaging over one month yielded a higher resolution image of the average plume transport than could be seen in the original swath data. During one episode, the volcano plume was clearly identified aloft but no impacts were detected at the surface, and on another day, the plume was split by the southeastern gap flow with part of it mixing down into the basin. Expanding the current analysis to a longer time period would show variations in the emission strengths and expanding it to a larger domain would identify regional transport and transformation of the plume.

The formation of sulfate aerosols is a clear application of this work, although it is not addressed here. Dunn et al. (2004) identified nucleation events during MCMA-2003 at both Santa Ana, a rural site, and CENICA, an urban site. These accompanied clean air events with high SO₂ concentrations and were particularly pronounced during periods of high relative humidity, as had already been described by Raga et al. (1999) and Baumgardner et al. (2000). The events took place during periods of northerly flow, where it is likely that the SO₂ transport was from the Tula complex (see also the hourly surface wind clusters for MCMA-2003 in the supplementary material <http://www.atmos-chem-phys.net/9/9599/2009/acp-9-9599-2009-supplement.pdf> of de Foy et al. (2008)).

During MILAGRO, Kleinman et al. (2008) identified sulfate formation rates within the polluted air mass that were consistent with Salcedo et al. (2006). On a more regional basis, three different SO₂ plumes with sulfate formation showed different ages and origins (DeCarlo et al., 2008), in accord with the present description of surface plumes from Tula mixing with the urban air mass and elevated plumes from the volcano. Future work could use the known plumes identified in this paper to explore aerosol formation measured during MILAGRO at both T0 and PTP.

SO₂ emissions from biomass burning could further impact the MCMA and especially sulfate aerosol formation Baumgardner et al. (2009). Estimates of the maximum total biomass emissions of SO₂ for the Yucatan during March 2006 are equivalent to emissions on the order of 5 kg/s based on Wiedinmyer et al. (2006) and would increase to 30 kg/s using the emission factors in Yokelson et al. (2009) making this source comparable to the volcano. Dilution would however be much larger for the Yucatan sources given their greater distance from the MCMA.

We have shown that SO₂ serves as a useful tracer for plume transport in the MCMA. It is hoped that this will facilitate interpretation of other measurements by comparing the behaviour of different species during the events, and additionally, by making use of similar analyses for different plumes. Maps of surface winds and of radar wind profiler data are provided in the supplementary material <http://www.atmos-chem-phys.net/9/9599/2009/acp-9-9599-2009-supplement.pdf> for this purpose.

Acknowledgements. We are indebted to the large number of people involved in the MILAGRO field campaign as well as those involved in monitoring in the Mexico City basin without which this study would not exist. We would like to thank A. Retama, C. Ortuño, M. Jaimes, G. Granados and the operators and analyst personnel of the “Red Automática de Monitoreo Atmosférico del Gobierno del Distrito Federal” for administering and gathering the surface air quality and meteorological data. M. Rosenhaus, J. L. Razo, J. Olalde and P. García of the Mexican National Meteorological Service kindly provided the EMA and radiosonde data. We are very grateful for the radar wind profiler data provided by S. J. Paech, D. Phillips and J. T. Walters of the University of

Alabama in Huntsville for T0 and by R. L. Coulter and T. J. Martin of Argonne National Laboratory for T1. We thank B. Lamb of Washington State University for the loan of the SO₂ monitor used aboard the Aerodyne mobile laboratory at PTP. We acknowledge the Goddard Earth Sciences Data and Information Services Center for providing the OMI data and J. E. Fritts for helpful discussions.

The MILAGRO field campaign was supported by the Comisión Ambiental Metropolitana of Mexico, NSF, DOE, NASA and USDA Forest Service among others. The financial support of the US National Science Foundation (awards ATM-0810931 and ATM-0810950) and the Molina Center for Strategic Studies in Energy and the Environment is gratefully acknowledged for this work.

Edited by: H. Singh

References

- Baumgardner, D., Raga, G. B., Kok, G., Ogren, J., Rosas, I., Baez, A., and Novakov, T.: On the evolution of aerosol properties at a mountain site above Mexico City, *J. Geophys. Res.*, 105, 22243–22253, 2000.
- Baumgardner, D., Grutter, M., Allan, J., Ochoa, C., Rappenglueck, B., Russell, L. M., and Arnott, P.: Physical and chemical properties of the regional mixed layer of Mexico’s Megapolis, *Atmos. Chem. Phys.*, 9, 5711–5727, 2009, <http://www.atmos-chem-phys.net/9/5711/2009/>.
- Bossert, J. E.: An investigation of flow regimes affecting the Mexico City region, *J. Appl. Meteorol.*, 36, 119–140, 1997.
- Boucher, A., Kyriakidis, P. C., and Cronkite-Ratcliff, C.: Geostatistical solutions for super-resolution land cover mapping, *IEEE T. Geosci. Remote Sens.*, 46, 272–283, doi:{10.1109/TGRS.2007.907102}, 2008.
- Capel, D.: *Image Mosaicing and Super-resolution*, Springer, 12–16, 2004.
- Carn, S. A., Krueger, A. J., Krotkov, N. A., Yang, K., and Levelt, P. F.: Sulfur dioxide emissions from Peruvian copper smelters detected by the Ozone Monitoring Instrument, *Geophys. Res. Lett.*, 34, L09801, doi:{10.1029/2006GL029020}, 2007.
- Chow, J. C., Watson, J. G., Edgerton, S. A., Vega, E., and Ortiz, E.: Spatial differences in outdoor PM₁₀ mass and aerosol composition in Mexico City, *J. Air Waste Manage. Assoc.*, 52, 423–434, 2002.
- Comisión Ambiental Metropolitana: *Inventario de Emisiones de la Zona Metropolitana del Valle de México*, Tech. Rep. (Web), Secretaría del Medio Ambiente, Gobierno de México, México, 2008.
- Corr, C. A., Krotkov, N., Madronich, S., Slusser, J. R., Holben, B., Gao, W., Flynn, J., Lefer, B., and Kreidenweis, S. M.: Retrieval of aerosol single scattering albedo at ultraviolet wavelengths at the T1 site during MILAGRO, *Atmos. Chem. Phys.*, 9, 5813–5827, 2009, <http://www.atmos-chem-phys.net/9/5813/2009/>.
- de Foy, B., Caetano, E., Magaña, V., Zitácuaro, A., Cárdenas, B., Retama, A., Ramos, R., Molina, L. T., and Molina, M. J.: Mexico City basin wind circulation during the MCMA-2003 field campaign, *Atmos. Chem. Phys.*, 5, 2267–2288, 2005, <http://www.atmos-chem-phys.net/5/2267/2005/>.

- de Foy, B., Clappier, A., Molina, L. T., and Molina, M. J.: Distinct wind convergence patterns in the Mexico City basin due to the interaction of the gap winds with the synoptic flow, *Atmos. Chem. Phys.*, 6, 1249–1265, 2006a.
- de Foy, B., Molina, L. T., and Molina, M. J.: Satellite-derived land surface parameters for mesoscale modelling of the Mexico City basin, *Atmos. Chem. Phys.*, 6, 1315–1330, 2006b.
- de Foy, B., Varela, J. R., Molina, L. T., and Molina, M. J.: Rapid ventilation of the Mexico City basin and regional fate of the urban plume, *Atmos. Chem. Phys.*, 6, 2321–2335, 2006c.
- de Foy, B., Lei, W., Zavala, M., Volkamer, R., Samuelsson, J., Melqvist, J., Galle, B., Martinez, A. P., Grutter, M., Retama, A., and Molina, L. T.: Modelling constraints on the emission inventory and on vertical dispersion for CO and SO₂ in the Mexico City Metropolitan Area using Solar FTIR and zenith sky UV spectroscopy, *Atmos. Chem. Phys.*, 7, 781–801, 2007, <http://www.atmos-chem-phys.net/7/781/2007/>.
- de Foy, B., Fast, J. D., Paech, S. J., Phillips, D., Walters, J. T., Coulter, R. L., Martin, T. J., Pekour, M. S., Shaw, W. J., Kasten-deuch, P. P., Marley, N. A., Retama, A., and Molina, L. T.: Basin-scale wind transport during the MILAGRO field campaign and comparison to climatology using cluster analysis, *Atmos. Chem. Phys.*, 8, 1209–1224, 2008, <http://www.atmos-chem-phys.net/8/1209/2008/>.
- de Foy, B., Zavala, M., Bei, N., and Molina, L. T.: Evaluation of WRF mesoscale simulations and particle trajectory analysis for the MILAGRO field campaign, *Atmos. Chem. Phys.*, 9, 4419–4438, 2009, <http://www.atmos-chem-phys.net/9/4419/2009/>.
- DeCarlo, P. F., Dunlea, E. J., Kimmel, J. R., Aiken, A. C., Sueper, D., Crouse, J., Wennberg, P. O., Emmons, L., Shinozuka, Y., Clarke, A., Zhou, J., Tomlinson, J., Collins, D. R., Knapp, D., Weinheimer, A. J., Montzka, D. D., Campos, T., and Jimenez, J. L.: Fast airborne aerosol size and chemistry measurements above Mexico City and Central Mexico during the MILAGRO campaign, *Atmos. Chem. Phys.*, 8, 4027–4048, 2008.
- Delgado-Granados, H., Gonzalez, L. C., and Sanchez, N. P.: Sulfur dioxide emissions from Popocatepetl volcano (Mexico): case study of a high-emission rate, passively degassing erupting volcano, *J. Volcanol. Geotherm. Res.*, 108, 107–120, 2001.
- Doran, J. C., Barnard, J. C., Arnott, W. P., Cary, R., Coulter, R., Fast, J. D., Kassianov, E. I., Kleinman, L., Laulainen, N. S., Martin, T., Paredes-Miranda, G., Pekour, M. S., Shaw, W. J., Smith, D. F., Springston, S. R., and Yu, X. Y.: The T1-T2 study: evolution of aerosol properties downwind of Mexico City, *Atmos. Chem. Phys.*, 7, 1585–1598, 2007, <http://www.atmos-chem-phys.net/7/1585/2007/>.
- Dunn, M., Jimenez, J., Baumgardner, D., Castro, T., McMurry, P., and Smith, J.: Measurements of Mexico City nanoparticle size distributions: Observations of new particle formation and growth, *Geophys. Res. Lett.*, 31, L10102, doi:{10.1029/2004GL019483}, 2004.
- ENVIRON: CAMx, comprehensive air quality model with extensions, User's Guide, Tech. Rep. Version 4.50, ENVIRON International Corporation, 2008.
- Fast, J. D. and Zhong, S. Y.: Meteorological factors associated with inhomogeneous ozone concentrations within the Mexico City basin, *J. Geophys. Res.-Atmos.*, 103, 18927–18946, 1998.
- Fast, J. D., de Foy, B., Rosas, F. A., Caetano, E., Carmichael, G., Emmons, L., McKenna, D., Mena, M., Skamarock, W., Tie, X., Coulter, R. L., Barnard, J. C., Wiedinmyer, C., and Madronich, S.: A meteorological overview of the MILAGRO field campaigns, *Atmos. Chem. Phys.*, 7, 2233–2257, 2007, <http://www.atmos-chem-phys.net/7/2233/2007/>.
- Grutter, M., Basaldud, R., Rivera, C., Harig, R., Junkerman, W., Caetano, E., and Delgado-Granados, H.: SO₂ emissions from Popocatepetl volcano: emission rates and plume imaging using optical remote sensing techniques, *Atmos. Chem. Phys.*, 8, 6655–6663, 2008, <http://www.atmos-chem-phys.net/8/6655/2008/>.
- Hong, S. Y., Noh, Y., and Dudhia, J.: A new vertical diffusion package with an explicit treatment of entrainment processes, *Mon. Weather Rev.*, 134, 2318–2341, 2006.
- Jauregui, E.: Local wind and air pollution interaction in the Mexico basin, *Atmosfera*, 1, 131–140, 1988.
- Jazcilevich, A. D., Garcia, A. R., and Caetano, E.: Locally induced surface air confluence by complex terrain and its effects on air pollution in the valley of Mexico, *Atmos. Environ.*, 39, 5481–5489, 2005.
- Jimenez, J. C., Raga, G. B., Baumgardner, D., Castro, T., Rosas, I., Baez, A., and Morton, O.: On the composition of airborne particles influenced by emissions of the volcano Popocatepetl in Mexico, *Nat. Hazards*, 31, 21–37, 2004.
- Juarez, A., Gay, C., and Flores, Y.: Impact of the Popocatepetl's volcanic activity on the air quality of Puebla City, Mexico, *Atmosfera*, 18, 57–69, 2005.
- Kain, J. S.: The Kain-Fritsch convective parameterization: An update, *J. Appl. Meteorol.*, 43, 170–181, 2004.
- Khokhar, M., Frankenberg, C., Van Roozendaal, M., Beirle, S., Kuhl, S., Richter, A., Platt, U., and Wagner, T.: Satellite observations of atmospheric SO₂ from volcanic eruptions during the time-period of 1996–2002, *Adv. Space Res.*, 36, 879–887, doi:{10.1016/j.asr.2005.04.114}, 2005.
- Kleinman, L. I., Springston, S. R., Daum, P. H., Lee, Y. N., Nunnemacker, L. J., Senum, G. I., Wang, J., Weinstein-Lloyd, J., Alexander, M. L., Hubbe, J., Ortega, J., Canagaratna, M. R., and Jayne, J.: The time evolution of aerosol composition over the Mexico City plateau, *Atmos. Chem. Phys.*, 8, 1559–1575, 2008, <http://www.atmos-chem-phys.net/8/1559/2008/>.
- Kolb, C. E., Herndon, S. C., McManus, B., Shorter, J. H., Zahniser, M. S., Nelson, D. D., Jayne, J. T., Canagaratna, M. R., and Worsnop, D. R.: Mobile laboratory with rapid response instruments for real-time measurements of urban and regional trace gas and particulate distributions and emission source characteristics, *Environ. Sci. Technol.*, 38, 5694–5703, 2004.
- Krotkov, N., Carn, S., Krueger, A., Bhartia, P., and Yang, K.: Band residual difference algorithm for retrieval of SO₂ from the aura Ozone Monitoring Instrument (OMI), *IEEE T. Geosci. Remote Sens.*, 44, 1259–1266, doi:{10.1109/TGRS.2005.861932}, 2006.
- Krotkov, N. A., McClure, B., Dickerson, R. R., Carn, S. A., Li, C., Bhartia, P. K., Yang, K., Krueger, A. J., Li, Z., Levelt, P. F., Chen, H., Wang, P., and Lu, D.: Validation of SO₂ retrievals from the Ozone Monitoring Instrument over NE China, *J. Geophys. Res.-Atmos.*, 113, doi:10.1029/2007JD008818, 2008.
- Li, F., Jia, X., and Fraser, D.: Superresolution Reconstruction of Multispectral Data for Improved Image Classification, *IEEE T. Geosci. Remote Sens.*, 6, 689–693, doi:{10.1109/LGRS.2009.2023604}, 2009.

- Loyola, D., van Geffen, J., Erbertseder, T., Roozendaal, M. V., Thomas, W., Zimmer, W., and Wisskirchen, K.: Satellite-based detection of volcanic sulphur dioxide from recent eruptions in Central and South America, *Adv. Geosci.*, 14, 35–40, 2008, <http://www.adv-geosci.net/14/35/2008/>.
- Marquez, C., Castro, T., Muhlia, A., Moya, M., Martinez-Arroyo, A., and Baez, A.: Measurement of aerosol particles, gases and flux radiation in the Pico de Orizaba National Park, and its relationship to air pollution transport, *Atmos. Environ.*, 39, 3877–3890, 2005.
- Molina, L. T., Kolb, C. E., de Foy, B., Lamb, B. K., Brune, W. H., Jimenez, J. L., Ramos-Villegas, R., Sarmiento, J., Paramo-Figueroa, V. H., Cardenas, B., Gutierrez-Avedoy, V., and Molina, M. J.: Air quality in North America's most populous city – overview of the MCMA-2003 campaign, *Atmos. Chem. Phys.*, 7, 2447–2473, 2007, <http://www.atmos-chem-phys.net/7/2447/2007/>.
- Moya, M., Castro, T., Zepeda, M., and Baez, A.: Characterization of size-differentiated inorganic composition of aerosols in Mexico City, *Atmos. Environ.*, 37, 3581–3591, 2003.
- O'Brien, J. J.: A note on the vertical structure of the eddy exchange coefficient in the planetary boundary layer, *J. Atmos. Sci.*, 27, 1214–1215, 1970.
- OMI Team: Ozone Monitoring Instrument (OMI) Data User's Guide, Tech. Rep. OMI-DUG-3.0, NASA, http://so2.umbc.edu/omi/omi_docs.html, 2009.
- Oreskes, N.: Evaluation (not validation) of quantitative models, *Environ. Health Perspect.*, 106, 1453–1460, 1998.
- Pyle, D. M. and Mather, T. A.: The regional influence of volcanic emissions from Popocatepetl, Mexico: Discussion of "Measurement of aerosol particles, gases and flux radiation in the Pico de Orizaba National Park, and its relationship to air pollution transport", Marquez et al., 2005, *Atmos. Environ.*, 39, 3877–3890, *Atmos. Environ.*, 39, 6475–6478, 2005.
- Raga, G. B., Kok, G. L., Baumgardner, D., Baez, A., and Rosas, I.: Evidence for volcanic influence on Mexico City aerosols, *Geophys. Res. Lett.*, 26, 1149–1152, 1999.
- Rivera, C., Sosa, G., Wöhrnschimmel, H., de Foy, B., Johansson, M., and Galle, B.: Tula industrial complex (Mexico) emissions of SO₂ and NO₂ during the MCMA 2006 field campaign using a mobile mini-DOAS system, *Atmos. Chem. Phys.*, 9, 6351–6361, 2009, <http://www.atmos-chem-phys.net/9/6351/2009/>.
- Salcedo, D., Onasch, T., Dzepina, K., Canagaratna, M., Zhang, Q., Huffman, J., DeCarlo, P., Jayne, J., Mortimer, P., Worsnop, D., Kolb, C., Johnson, K., Zuberi, B., Marr, L., Volkamer, R., Molina, L., Molina, M., Cardenas, B., Bernabe, R., Marquez, C., Gaffney, J., Marley, N., Laskin, A., Shutthanandan, V., Xie, Y., Brune, W., Leshner, R., Shirley, T., and Jimenez, J.: Characterization of ambient aerosols in Mexico City during the MCMA-2003 campaign with Aerosol Mass Spectrometry: results from the CENICA Supersite, *Atmos. Chem. Phys.*, 6, 925–946, 2006, <http://www.atmos-chem-phys.net/6/925/2006/>.
- Secretaría del Medio Ambiente del Gobierno del Distrito Federal: Inventario de Emisiones de Contaminantes Criterio de la Zona Metropolitana del Valle de México, Tech. Rep. (Web), Secretaría del Medio Ambiente, Gobierno del Distrito Federal, México, 2008.
- Skamarock, W. C., Klemp, J. B., Dudhia, J., Gill, D. O., Barker, D. M., Wang, W., and Powers, J. G.: A Description of the Advanced Research WRF Version 2, Tech. Rep. NCAR/TN-468+STR, NCAR, 2005.
- Taylor, K. E.: Summarizing multiple aspects of model performance in a single diagram., *J. Geophys. Res.-Atmos.*, 106, 7183–7192, 2001.
- Wiedinmyer, C., Quayle, B., Geron, C., Belote, A., McKenzie, D., Zhang, X., O'Neill, S., and Wynne, K. K.: Estimating emissions from fires in North America for air quality modeling, *Atmos. Environ.*, 40, 3419–3432, doi:{10.1016/j.atmosenv.2006.02.010}, 2006.
- Williams, M. D., Brown, M. J., Cruz, X., Sosa, G., and Streit, G.: Development and testing of meteorology and air dispersion models for Mexico City, *Atmos. Environ.*, 29(21), 2929–2960, 1995.
- Willmott, C. J.: Some comments on the evaluation of model performance, *B. Am. Meteor. Soc.*, 63, 1309–1313, 1982.
- Yang, K., Krotkov, N. A., Krueger, A. J., Carn, S. A., Bhartia, P. K., and Levelt, P. F.: Retrieval of large volcanic SO₂ columns from the Aura Ozone Monitoring Instrument: Comparison and limitations, *J. Geophys. Res.-Atmos.*, 112, D24S43, doi:{10.1029/2007JD008825}, 2007.
- Yang, K., Krotkov, N. A., Krueger, A. J., Carn, S. A., Bhartia, P. K., and Levelt, P. F.: Improving retrieval of volcanic sulfur dioxide from backscattered UV satellite observations, *Geophys. Res. Lett.*, 36, L03102, doi:{10.1029/2008GL036036}, 2009.
- Yokelson, R. J., Crounse, J. D., DeCarlo, P. F., Karl, T., Urbanski, S., Atlas, E., Campos, T., Shinozuka, Y., Kapustin, V., Clarke, A. D., Weinheimer, A., Knapp, D. J., Montzka, D. D., Holloway, J., Weibring, P., Flocke, F., Zheng, W., Toohey, D., Wennberg, P. O., Wiedinmyer, C., Mauldin, L., Fried, A., Richter, D., Walega, J., Jimenez, J. L., Adachi, K., Buseck, P. R., Hall, S. R., and Shetter, R.: Emissions from biomass burning in the Yucatan, *Atmos. Chem. Phys.*, 9, 5785–5812, 2009, <http://www.atmos-chem-phys.net/9/5785/2009/>.
- Zängl, G., Chimani, B., and Häberli, C.: Numerical Simulations of the Foehn in the Rhine Valley on 24 October 1999 (MAP IOP 10), *Mon. Weather Rev.*, 132, 368–389, 2004.